

Higgs boson decay $h \rightarrow Z\gamma$ and muon magnetic dipole moment in the $\mu\nu$ SSM

Chang-Xin Liu^{a,b*}, Hai-Bin Zhang^{a,b†}, Jin-Lei Yang^{a,b,c‡},
Shu-Min Zhao^{a,b§}, Yu-Bin Liu^d, Tai-Fu Feng^{a,b,e¶}

^a*Department of Physics, Hebei University, Baoding, 071002, China*

^b*Key Laboratory of High-precision Computation and Application of Quantum Field Theory of Hebei Province, Baoding, 071002, China*

^c*Institute of theoretical Physics, Chinese Academy of Sciences, Beijing, 100190, China*

^d*School of Physics, Nankai University, Tianjin 300071, China*

^e*College of Physics, Chongqing University, Chongqing, 400044, China*

Abstract

To solve the μ problem and generate three tiny neutrino masses in the MSSM, the μ from ν Supersymmetric Standard Model ($\mu\nu$ SSM), introduces three singlet right-handed neutrino superfields, which lead to the mixing of the Higgs doublets with the sneutrinos. The mixing affects the lightest Higgs boson mass and the Higgs couplings. The present observed 95% CL upper limit on signal strength of 125 GeV Higgs boson decay to $Z\gamma$ is 6.6, which still is plenty of space to prove the existence of new physics. In this work, we investigate the signal strength of the 125 GeV Higgs boson decay channel $h \rightarrow Z\gamma$ in the $\mu\nu$ SSM. Besides, we consider the two-loop electroweak corrections of muon anomalous magnetic dipole moment (MDM) in the model, which also make important contributions compared with one-loop electroweak corrections.

PACS numbers: 12.60.Jv, 14.80.Da

Keywords: Supersymmetry, Higgs boson decay, Muon MDM

* LIUchangxinZ@163.com

† hbzhang@hbu.edu.cn

‡ JLYangJL@163.com

§ zhaosm@hbu.edu.cn

¶ fengtf@hbu.edu.cn

I. INTRODUCTION

A great success of the Large Hadron Collider (LHC) is the discovery of the Higgs boson [1, 2]. Combining the updated data [3–5], the measured mass of the Higgs boson now is [6]

$$m_h = 125.10 \pm 0.14 \text{ GeV}. \quad (1)$$

Therefore, the accurate Higgs boson mass gives most stringent constraint on parameter space for the standard model and its various extensions. The next step is focusing on searching for the properties of the Higgs boson. Now, the signal strengths for the Higgs boson decays $h \rightarrow \gamma\gamma$, $h \rightarrow VV^*$ ($V = Z, W$) and $h \rightarrow f\bar{f}$ ($f = b, \tau$) can be detected precise values. The signal strength for their combined final states is 1.10 ± 0.11 [6], which is consistent with the value of the standard model (SM) in the error range. The LHC also has reported the searches for the rare decay process $h \rightarrow Z\gamma$ [7–10]. But No evidence for the $h \rightarrow Z\gamma$ decay is observed and the present observed 95% CL upper limit on its signal strength is 6.6 [9]. So, for decay $h \rightarrow Z\gamma$, there is still plenty of space for new physics (NP). Within various theoretical frameworks, the Higgs boson decay $h \rightarrow Z\gamma$ has been discussed [11–42].

As one of the candidates of new physics, the μ from ν supersymmetric standard model ($\mu\nu$ SSM) [43–49] can solve the μ problem [50] of the minimal supersymmetric standard model (MSSM) [51–55] through introducing three singlet right-handed neutrino superfields $\hat{\nu}_i^c$ ($i = 1, 2, 3$). The neutrino superfields lead the mixing of the neutral components of the Higgs doublets with the sneutrinos, which is different from the Higgs sector of the MSSM. In our previous work, the Higgs boson decay modes $h \rightarrow \gamma\gamma$, $h \rightarrow VV^*$ ($V = Z, W$), $h \rightarrow f\bar{f}$ ($f = b, \tau$), $h \rightarrow \mu\tau$, and the masses of the Higgs bosons in the $\mu\nu$ SSM have been researched [56–58]. In this paper, we will investigate the 125 GeV Higgs boson decay channel $h \rightarrow Z\gamma$ in the $\mu\nu$ SSM.

The current difference between the experimental measurement [59] and SM theoretical prediction of the muon anomaly magnetic dipole moment (MDM) [6],

$$\Delta a_\mu = a_\mu^{exp} - a_\mu^{SM} = (26.8 \pm 7.7) \times 10^{-10}, \quad (2)$$

represents an interesting but not yet conclusive discrepancy of 3.5 standard deviation, which still stands as a potential indication of the existence of new physics. Several predictions for

the muon anomaly MDM have been discussed in the framework of various SM extensions [60–75]. In the $\mu\nu$ SSM, we have studied the muon MDM at one-loop level [57]. In this work, we will consider the two-loop Barr-Zee type diagrams of the muon anomaly MDM in the framework of the $\mu\nu$ SSM.

The paper is organized as follows. In Sec. II, we introduce the $\mu\nu$ SSM briefly, about the superpotential and the soft SUSY-breaking terms. In Sec. III, we give the decay width and the signal strength of $h \rightarrow Z\gamma$. Sec. IV includes the two-loop electroweak corrections of the muon anomaly MDM. Sec. V and Sec. VI respectively show the numerical analysis and summary. Some formulae are collected in Appendix.

II. THE $\mu\nu$ SSM

In addition to the MSSM Yukawa couplings for quarks and charged leptons, the superpotential of the $\mu\nu$ SSM contains Yukawa couplings for neutrinos, two additional types of terms involving the Higgs doublet superfields \hat{H}_u and \hat{H}_d , and the right-handed neutrino superfields $\hat{\nu}_i^c$, [43]

$$\begin{aligned}
W = & \epsilon_{ab} \left(Y_{u_{ij}} \hat{H}_u^b \hat{Q}_i^a \hat{u}_j^c + Y_{d_{ij}} \hat{H}_d^a \hat{Q}_i^b \hat{d}_j^c + Y_{e_{ij}} \hat{H}_d^a \hat{L}_i^b \hat{e}_j^c \right) \\
& + \epsilon_{ab} Y_{\nu_{ij}} \hat{H}_u^b \hat{L}_i^a \hat{\nu}_j^c - \epsilon_{ab} \lambda_i \hat{\nu}_i^c \hat{H}_d^a \hat{H}_u^b + \frac{1}{3} \kappa_{ijk} \hat{\nu}_i^c \hat{\nu}_j^c \hat{\nu}_k^c,
\end{aligned} \tag{3}$$

where $\hat{H}_u^T = (\hat{H}_u^+, \hat{H}_u^0)$, $\hat{H}_d^T = (\hat{H}_d^0, \hat{H}_d^-)$, $\hat{Q}_i^T = (\hat{u}_i, \hat{d}_i)$, $\hat{L}_i^T = (\hat{\nu}_i, \hat{e}_i)$ (the index T denotes the transposition) represent $SU(2)$ doublet superfields, and \hat{u}_i^c , \hat{d}_i^c , and \hat{e}_i^c are the singlet up-type quark, down-type quark and charged lepton superfields, respectively. In addition, $Y_{u,d,e,\nu}$, λ , and κ are dimensionless matrices, a vector, and a totally symmetric tensor. $a, b = 1, 2$ are $SU(2)$ indices with antisymmetric tensor $\epsilon_{12} = 1$, and $i, j, k = 1, 2, 3$ are generation indices. The summation convention is implied on repeated indices in the following.

In the superpotential, if the scalar potential is such that nonzero VEVs of the scalar components ($\tilde{\nu}_i^c$) of the singlet neutrino superfields $\hat{\nu}_i^c$ are induced, the effective bilinear terms $\epsilon_{ab} \varepsilon_i \hat{H}_u^b \hat{L}_i^a$ and $\epsilon_{ab} \mu \hat{H}_d^a \hat{H}_u^b$ are generated, with $\varepsilon_i = Y_{\nu_{ij}} \langle \tilde{\nu}_j^c \rangle$ and $\mu = \lambda_i \langle \tilde{\nu}_i^c \rangle$, once the electroweak symmetry is broken. The last term generates the effective Majorana masses for neutrinos at the electroweak scale. Therefore, the $\mu\nu$ SSM can generate three tiny neutrino

masses at the tree level through TeV scale seesaw mechanism [44, 76–82].

In supersymmetric (SUSY) extensions of the standard model, the R-parity of a particle is defined as $R = (-1)^{L+3B+2S}$ [51–55]. R-parity is violated if either the baryon number (B) or lepton number (L) is not conserved, where S denotes the spin of concerned component field. The last two terms in Eq. (3) explicitly violate lepton number and R-parity. R-parity breaking implies that the lightest supersymmetric particle (LSP) is no longer stable. In this context, the neutralino or the sneutrino are no longer candidates for the dark matter (DM). However, other SUSY particles such as the gravitino or the axino can still be used as candidates [44, 45, 79, 83–88].

The dark matter candidate must be stable on the cosmic timescale, so that it is still around today [89]. In Refs. [83–86], the authors analyzed the gravitino dark matter candidate in the $\mu\nu$ SSM, whose lifetime is long lived compared to the current age of the Universe. The gravitino turns out to be an interesting candidate for DM, which may be searched through gamma-ray observations with Fermi-LAT. Recently, the axino dark matter candidate in the $\mu\nu$ SSM also be analyzed [87, 88].

The general soft SUSY-breaking terms of the $\mu\nu$ SSM are given by

$$\begin{aligned}
-\mathcal{L}_{soft} = & m_{\tilde{Q}_{ij}}^2 \tilde{Q}_i^{a*} \tilde{Q}_j^a + m_{\tilde{u}_{ij}^c}^2 \tilde{u}_i^{c*} \tilde{u}_j^c + m_{\tilde{d}_{ij}^c}^2 \tilde{d}_i^{c*} \tilde{d}_j^c + m_{\tilde{L}_{ij}}^2 \tilde{L}_i^{a*} \tilde{L}_j^a \\
& + m_{\tilde{e}_{ij}^c}^2 \tilde{e}_i^{c*} \tilde{e}_j^c + m_{H_d}^2 H_d^{a*} H_d^a + m_{H_u}^2 H_u^{a*} H_u^a + m_{\tilde{\nu}_{ij}^c}^2 \tilde{\nu}_i^{c*} \tilde{\nu}_j^c \\
& + \epsilon_{ab} \left[(A_u Y_u)_{ij} H_u^b \tilde{Q}_i^a \tilde{u}_j^c + (A_d Y_d)_{ij} H_d^a \tilde{Q}_i^b \tilde{d}_j^c + (A_e Y_e)_{ij} H_d^a \tilde{L}_i^b \tilde{e}_j^c + \text{H.c.} \right] \\
& + \left[\epsilon_{ab} (A_\nu Y_\nu)_{ij} H_u^b \tilde{L}_i^a \tilde{\nu}_j^c - \epsilon_{ab} (A_\lambda \lambda)_i \tilde{\nu}_i^c H_d^a H_u^b + \frac{1}{3} (A_\kappa \kappa)_{ijk} \tilde{\nu}_i^c \tilde{\nu}_j^c \tilde{\nu}_k^c + \text{H.c.} \right] \\
& - \frac{1}{2} \left(M_3 \tilde{\lambda}_3 \tilde{\lambda}_3 + M_2 \tilde{\lambda}_2 \tilde{\lambda}_2 + M_1 \tilde{\lambda}_1 \tilde{\lambda}_1 + \text{H.c.} \right). \tag{4}
\end{aligned}$$

Here, the first two lines contain mass squared terms of squarks, sleptons, and Higgses. The next two lines consist of the trilinear scalar couplings. In the last line, M_3 , M_2 , and M_1 denote Majorana masses corresponding to $SU(3)$, $SU(2)$, and $U(1)$ gauginos $\hat{\lambda}_3$, $\hat{\lambda}_2$, and $\hat{\lambda}_1$, respectively. In addition to the terms from \mathcal{L}_{soft} , the tree-level scalar potential receives the usual D - and F -term contributions [44, 45].

Once the electroweak symmetry is spontaneously broken, the neutral scalars develop in

general the VEVs:

$$\langle H_d^0 \rangle = v_d, \quad \langle H_u^0 \rangle = v_u, \quad \langle \tilde{\nu}_i \rangle = v_{\nu_i}, \quad \langle \tilde{\nu}_i^c \rangle = v_{\nu_i^c}. \quad (5)$$

One can define the neutral scalars as

$$\begin{aligned} H_d^0 &= \frac{h_d + iP_d}{\sqrt{2}} + v_d, & \tilde{\nu}_i &= \frac{(\tilde{\nu}_i)^{\Re} + i(\tilde{\nu}_i)^{\Im}}{\sqrt{2}} + v_{\nu_i}, \\ H_u^0 &= \frac{h_u + iP_u}{\sqrt{2}} + v_u, & \tilde{\nu}_i^c &= \frac{(\tilde{\nu}_i^c)^{\Re} + i(\tilde{\nu}_i^c)^{\Im}}{\sqrt{2}} + v_{\nu_i^c}, \end{aligned} \quad (6)$$

and

$$\tan \beta = \frac{v_u}{v_d}. \quad (7)$$

In the $\mu\nu$ SSM, the left- and right-handed sneutrino VEVs lead to the mixing of the neutral components of the Higgs doublets with the sneutrinos producing an 8×8 CP-even neutral scalar mass matrix, which can be seen in Refs. [44, 45, 48]. The mixing gives a rich phenomenology in the Higgs sector of the $\mu\nu$ SSM. In the large m_A limit, we give an approximate expression for the lightest Higgs boson mass [58],

$$m_h^2 \approx \xi_h m_{H_1}^2, \quad (8)$$

where

$$m_{H_1}^2 \simeq m_Z^2 \cos 2\beta^2 + \frac{2\lambda_i \lambda_i s_W^2 c_W^2}{e^2} m_Z^2 \sin 2\beta + \Delta m_{H_1}^2, \quad (9)$$

and ξ_h comes from the mixing of the Higgs doublets with the sneutrinos, which concrete expression can be found in Ref. [58]. Comparing with the MSSM, the $\mu\nu$ SSM gets an additional term $\frac{2\lambda_i \lambda_i s_W^2 c_W^2}{e^2} m_Z^2 \sin 2\beta$. The radiative corrections $\Delta m_{H_1}^2$ can be computed more precisely by some public tools, for example, FeynHiggs [90–97], SOFTSUSY [98–100], SPheno [101, 102], and so on. In the following numerical section, we will use the FeynHiggs-2.13.0 to calculate the radiative corrections for the Higgs boson mass about the MSSM part.

III. THE RARE DECAY $h \rightarrow Z\gamma$

The $h \rightarrow Z\gamma$ coupling in the SM is similar to the $h \rightarrow \gamma\gamma$ coupling, which is built up by the heavy top quark and W boson loops [16]. In the supersymmetric models of the SM, there are more kind of particle makes contributions to the LO decay width, W boson, the third-generation fermions ($f = t, b, \tau$) and the supersymmetric partners [17]. In the framework of the $\mu\nu$ SSM, the decay width of the loop induced Higgs boson decay $h \rightarrow Z\gamma$ can be given as

$$\begin{aligned} \Gamma_{\text{NP}}(h \rightarrow Z\gamma) &= \frac{\alpha G_F^2 m_W^2 m_h^3}{64\pi^4} \left(1 - \frac{m_Z^2}{m_h^2}\right)^3 \left| \sum_{f=t,b,\tau} Q_f N_f \hat{v}_f g_{hff} A_{1/2}(x_f, \lambda_f) + g_{hWW} A_1(x_W, \lambda_W) \right. \\ &\quad + (2c_W^2 - 1) g_{hS_\alpha^\pm S_\alpha^-} \frac{m_Z^2}{m_{S_\alpha^\pm}^2} A_0(x_{S_\alpha^\pm}, \lambda_{S_\alpha^\pm}) + \sum_{\tilde{f}=U_I^+, D_I^-} N_c Q_{\tilde{f}} \hat{v}_{\tilde{f}} g_{h\tilde{f}\tilde{f}} \frac{m_Z^2}{m_{\tilde{f}}^2} A_0(x_{\tilde{f}}, \lambda_{\tilde{f}}) \\ &\quad \left. + \sum_{m,n=L,R} g_{h\chi_i\chi_i}^m g_{Z\chi_i\chi_i}^n \frac{2m_W}{m_{\chi_i}} A_{1/2}(x_{\chi_i}, \lambda_{\chi_i}) \right|^2, \end{aligned} \quad (10)$$

with $x_i = 4m_i^2/m_h^2$, $\lambda_i = 4m_i^2/m_Z^2$, $\hat{v}_f = (2I_f^3 - 4Q_f s_W^2)/c_W$, $\hat{v}_{\tilde{f}_1} = (I_f^3 \cos^2 \theta_f - Q_f s_W^2)/c_W$, $\hat{v}_{\tilde{f}_2} = (I_f^3 \sin^2 \theta_f - Q_f s_W^2)/c_W$, θ_f is the mixing angle of sfermions $\tilde{f}_{1,2}$. The form factors A_0 , $A_{1/2}$ and A_1 are showed in Appendix A. The concrete expressions of g_{hff} , g_{hWW} , $g_{hS_\alpha^\pm S_\alpha^-}$, $g_{h\tilde{f}\tilde{f}}$ can be found in Ref [56]. And the expressions of $g_{Z\chi_i\chi_i}^n$ and $g_{h\chi_i\chi_i}^n$ are

$$g_{Z\chi_i\chi_i}^n = -\frac{1}{e} C_n^{Z\chi_i\bar{\chi}_i}, \quad g_{h\chi_i\chi_i}^n = -\frac{1}{e} C_n^{S_1\chi_i\bar{\chi}_i} \quad (n = L, R), \quad (11)$$

where $C_n^{Z\chi_i\bar{\chi}_i}$ and $C_n^{S_1\chi_i\bar{\chi}_i}$ ($h = S_1$) can be seen in Ref. [48].

The decay width of $h \rightarrow Z\gamma$ at leading order (LO) in the $\mu\nu$ SSM are mediated by charged heavy particle loops built up by W bosons, standard fermions f , charged scalars S_α^\pm , charginos χ_i and sfermions \tilde{f} . When the supersymmetric particles are more heavy, the contributions of supersymmetric particles will be small. The signal strength of Higgs boson decay $h \rightarrow Z\gamma$ is a physical quantity that can be observed directly, and it can written by

$$\mu_{Z\gamma}^{\text{ggF}} = \frac{\sigma_{\text{NP}}(\text{ggF})}{\sigma_{\text{SM}}(\text{ggF})} \frac{\text{BR}_{\text{NP}}(h \rightarrow Z\gamma)}{\text{BR}_{\text{SM}}(h \rightarrow Z\gamma)}, \quad (12)$$

normalized to the SM values, where ggF stands for gluon-gluon fusion. One can evaluate the Higgs production cross sections

$$\frac{\sigma_{\text{NP}}(\text{ggF})}{\sigma_{\text{SM}}(\text{ggF})} \approx \frac{\Gamma_{\text{NP}}(h \rightarrow gg)}{\Gamma_{\text{SM}}(h \rightarrow gg)} = \frac{\Gamma_{\text{NP}}^h}{\Gamma_{\text{SM}}^h} \frac{\Gamma_{\text{NP}}(h \rightarrow gg)/\Gamma_{\text{NP}}^h}{\Gamma_{\text{SM}}(h \rightarrow gg)/\Gamma_{\text{SM}}^h}$$

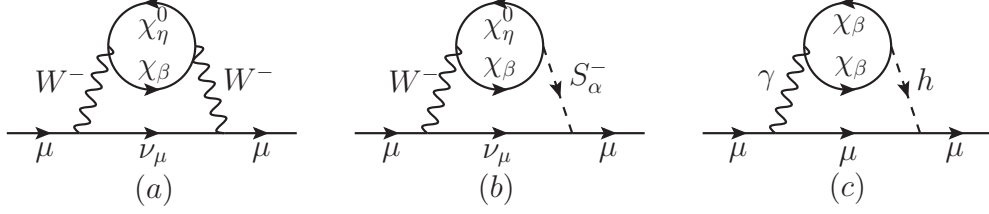


FIG. 1: The main two-loop Barr-Zee type diagrams in which a closed fermion loop is attached to the virtual gauge bosons or Higgs fields, the corresponding contributions to the muon MDM are obtained by attaching a photon on all possible ways to the internal particles.

$$= \frac{\Gamma_{\text{NP}}^h}{\Gamma_{\text{SM}}^h} \frac{\text{BR}_{\text{NP}}(h \rightarrow gg)}{\text{BR}_{\text{SM}}(h \rightarrow gg)}, \quad (13)$$

and the total decay width of the 125 GeV Higgs boson in the NP is [56]

$$\begin{aligned} \Gamma_{\text{NP}}^h \simeq & \sum_{f=b,\tau,c,s} \Gamma_{\text{NP}}(h \rightarrow f\bar{f}) + \sum_{V=Z,W} \Gamma_{\text{NP}}(h \rightarrow VV^*) \\ & + \Gamma_{\text{NP}}(h \rightarrow gg) + \Gamma_{\text{NP}}(h \rightarrow \gamma\gamma) + \Gamma_{\text{NP}}(h \rightarrow Z\gamma), \end{aligned} \quad (14)$$

where we neglected the little contribution which is rare or invisible, and the Γ_{SM}^h is the total decay width of the SM Higgs boson. Through Eqs. (12-14), we can quantify the signal strength for the Higgs boson decay channel $h \rightarrow Z\gamma$ in the $\mu\nu\text{SSM}$.

IV. TWO-LOOP CORRECTIONS OF MUON MDM

The muon MDM in the $\mu\nu\text{SSM}$ can be given as the effective Lagrangian

$$\mathcal{L}_{MDM} = \frac{e}{4m_\mu} a_\mu \bar{l}_\mu \sigma^{\alpha\beta} l_\mu F_{\alpha\beta}, \quad (15)$$

where l_μ denotes the muon which is on-shell, m_μ is the mass of the muon, $\sigma^{\alpha\beta} = \frac{i}{2}[\gamma^\alpha, \gamma^\beta]$, $F_{\alpha\beta}$ represents the electromagnetic field strength and muon MDM, $a_\mu = \frac{1}{2}(g-2)_\mu$. Including two-loop electroweak corrections, the muon MDM in the $\mu\nu\text{SSM}$ can be written by

$$a_\mu^{SUSY} = a_\mu^{one-loop} + a_\mu^{two-loop}, \quad (16)$$

where the one-loop corrections $a_\mu^{one-loop}$ can be found in Ref. [57].

The two-loop Barr-Zee type diagrams can give important contributions to the muon MDM in a reasonable parameter space. According to Ref. [70, 74], the main two-loop Barr-Zee

type diagrams contributing to the muon MDM in the $\mu\nu$ SSM are shown in Fig. 1. Here, we ignore some two-loop diagrams which have low contributions, due to the decoupling theorem. In the $\mu\nu$ SSM, the two-loop corrections are given as

$$a_\mu^{two-loop} = a_\mu^{WW} + a_\mu^{WS} + a_\mu^{\gamma h}, \quad (17)$$

where the terms $a_\mu^{WW}, a_\mu^{WS}, a_\mu^{\gamma h}$ are the contributions corresponding to Fig. 1 (a-c). Under the assumption $m_F = m_{\chi_\beta} \simeq m_{\chi_\eta^0} \gg m_W$, the concrete expression can be approximately written as

$$a_\mu^{WW} = \frac{G_F m_\mu^2}{192\sqrt{2}\pi^4} \{5(|C_L^{W\chi_\beta\bar{\chi}_\eta^0}|^2 + |C_R^{W\chi_\beta\bar{\chi}_\eta^0}|^2) - 6(|C_L^{W\chi_\beta\bar{\chi}_\eta^0}|^2 - |C_R^{W\chi_\beta\bar{\chi}_\eta^0}|^2) + 11\Re(C_L^{W\chi_\beta\bar{\chi}_\eta^0} C_R^{W\chi_\beta\bar{\chi}_\eta^0*})\}, \quad (18)$$

$$a_\mu^{WS} = \frac{G_F m_\mu m_W^2 \Re(C_L^{S_\alpha^- \chi_9^0 \bar{\chi}_4})}{128\pi^4 m_F g_2} \times \left\{ \left[\frac{179}{36} + \frac{10}{3} J(m_F^2, m_W^2, m_{S_\alpha^-}^2) \right] \Re(C_L^{W\chi_\beta\bar{\chi}_\eta^0} C_L^{W\chi_\beta\bar{\chi}_\eta^0} + C_R^{W\chi_\beta\bar{\chi}_\eta^0} C_R^{W\chi_\beta\bar{\chi}_\eta^0}) \right. \\ + \left[-\frac{1}{9} - \frac{2}{3} J(m_F^2, m_W^2, m_{S_\alpha^-}^2) \right] \Re(C_L^{W\chi_\beta\bar{\chi}_\eta^0} C_R^{W\chi_\beta\bar{\chi}_\eta^0} + C_R^{W\chi_\beta\bar{\chi}_\eta^0} C_L^{W\chi_\beta\bar{\chi}_\eta^0}) \\ + \left[-\frac{16}{9} - \frac{8}{3} J(m_F^2, m_W^2, m_{S_\alpha^-}^2) \right] \Re(C_L^{W\chi_\beta\bar{\chi}_\eta^0} C_L^{W\chi_\beta\bar{\chi}_\eta^0} - C_R^{W\chi_\beta\bar{\chi}_\eta^0} C_R^{W\chi_\beta\bar{\chi}_\eta^0}) \\ \left. + \left[-\frac{2}{9} - \frac{4}{3} J(m_F^2, m_W^2, m_{S_\alpha^-}^2) \right] \Re(C_L^{W\chi_\beta\bar{\chi}_\eta^0} C_R^{W\chi_\beta\bar{\chi}_\eta^0} - C_R^{W\chi_\beta\bar{\chi}_\eta^0} C_L^{W\chi_\beta\bar{\chi}_\eta^0}) \right\}, \quad (19)$$

$$a_\mu^{\gamma h} = \frac{-G_F m_\mu m_W^2}{32\pi^4 m_F} \left[1 + \ln \frac{m_F^2}{m_h^2} \right] \Re(C_L^{S_1 \chi_2 \bar{\chi}_2} C_L^{S_1 \chi_\beta \bar{\chi}_\beta}), \quad (20)$$

where

$$J(x, y, z) = \ln x - \frac{y \ln y - z \ln z}{y - z}. \quad (21)$$

Here, $\Re(\dots)$ represents the operation to take the real part of a complex number, the concrete expressions for couplings C can be found in Ref. [48].

V. NUMERICAL ANALYSIS

In the $\mu\nu$ SSM, there are many free parameters, we can take some appropriate parameter space, so that we can obtain a transparent numerical results. First, we make the minimal

flavor violation (MFV) assumptions for some parameters, which assume

$$\begin{aligned}
\kappa_{ijk} &= \kappa \delta_{ij} \delta_{jk}, & (A_\kappa \kappa)_{ijk} &= A_\kappa \kappa \delta_{ij} \delta_{jk}, & \lambda_i &= \lambda, \\
(A_\lambda \lambda)_i &= A_\lambda \lambda, & Y_{e_{ij}} &= Y_{e_i} \delta_{ij}, & (A_e Y_e)_{ij} &= A_e Y_{e_i} \delta_{ij}, \\
Y_{\nu_{ij}} &= Y_{\nu_i} \delta_{ij}, & (A_\nu Y_\nu)_{ij} &= a_{\nu_i} \delta_{ij}, & m_{\tilde{\nu}_i^c}^2 &= m_{\tilde{\nu}_i}^2 \delta_{ij}, \\
m_{\tilde{Q}_{ij}}^2 &= m_{\tilde{Q}_i}^2 \delta_{ij}, & m_{\tilde{u}_{ij}^c}^2 &= m_{\tilde{u}_i}^2 \delta_{ij}, & m_{\tilde{d}_{ij}^c}^2 &= m_{\tilde{d}_i}^2 \delta_{ij}, \\
m_{\tilde{L}_{ij}}^2 &= m_{\tilde{L}_i}^2 \delta_{ij}, & m_{\tilde{e}_{ij}^c}^2 &= m_{\tilde{e}_i}^2 \delta_{ij}, & \nu_{\nu_i^c} &= \nu_{\nu_i},
\end{aligned} \tag{22}$$

where $i, j, k = 1, 2, 3$. $m_{\tilde{\nu}_i^c}^2$ can be constrained by the minimization conditions of the neutral scalar potential seen in Ref. [58]. To agree with experimental observations on quark mixing, one can have

$$\begin{aligned}
Y_{u_{ij}} &= Y_{u_i} V_{L_{ij}}^u, & (A_u Y_u)_{ij} &= A_{u_i} Y_{u_{ij}}, \\
Y_{d_{ij}} &= Y_{d_i} V_{L_{ij}}^d, & (A_d Y_d)_{ij} &= A_{d_i} Y_{d_{ij}},
\end{aligned} \tag{23}$$

and $V = V_L^u V_L^{d\dagger}$ denotes the CKM matrix.

$$Y_{u_i} = \frac{m_{u_i}}{v_u}, \quad Y_{d_i} = \frac{m_{d_i}}{v_d}, \quad Y_{e_i} = \frac{m_{l_i}}{v_d}, \tag{24}$$

where the m_{u_i}, m_{d_i} and m_{l_i} stands for the up-quark, down-quark and charged lepton masses, and we can find the value of the masses from PDG [6]. Through our previous work [82], we have discussed in detail how the neutrino oscillation data constrain neutrino Yukawa couplings $Y_{\nu_i} \sim \mathcal{O}(10^{-7})$ and left-handed sneutrino VEVs $v_{\nu_i} \sim \mathcal{O}(10^{-4} \text{ GeV})$ in the $\mu\nu\text{SSM}$ via the TeV scale seesaw mechanism.

Through analysis of the parameter space of the $\mu\nu\text{SSM}$ in Ref. [44], we can take reasonable parameter values to be $\lambda = 0.1$, $\kappa = 0.4$, $A_\lambda = 500 \text{ GeV}$, $A_\kappa = -300 \text{ GeV}$ and $A_{u_{1,2}} = A_d = A_e = 1 \text{ TeV}$ for simplicity. Considering the direct search for supersymmetric particles [6], we take $m_{\tilde{Q}_{1,2,3}} = m_{\tilde{u}_{1,2}^c} = m_{\tilde{d}_{1,2,3}^c} = 2 \text{ TeV}$, $m_{\tilde{L}} = m_{\tilde{e}^c} = 1 \text{ TeV}$, $M_3 = 2.5 \text{ TeV}$. For simplicity, we will choose the gauginos' Majorana masses $M_1 = M_2$. As key parameters, $A_{u_3} = A_t$, $m_{\tilde{u}_3^c}$ and $\tan \beta$ greatly affect the lightest Higgs boson mass. Therefore, the free parameters that affect our next analysis are $\tan \beta$, v_{ν^c} , M_2 , $m_{\tilde{u}_3^c}$, and A_t .

In the supersymmetric model, there is a close similarity between the anomalous magnetic dipole moment of muon and the branching ratio of $\bar{B} \rightarrow X_s \gamma$, in that both get

Parameters	Min	Max	Step
$\tan \beta$	4	40	2
v_{ν^c}/TeV	1	14	0.5
$m_{\tilde{u}_3^c}/\text{TeV}$	1	4	0.3
A_t/TeV	1	4	0.3

TABLE I: Scanning parameters for the muon MDM with $M_2 = \mu \equiv 3\lambda v_{\nu^c}$.

large $\tan \beta$ enhancements from a Higgsino-sfermion-fermion interaction vertex with a down-fermion Yukawa coupling [63]. So in the following, we also consider the constraint from the branching ratio of $\bar{B} \rightarrow X_s \gamma$. The current combined experimental data for the branching ratio of $\bar{B} \rightarrow X_s \gamma$ measured by CLEO [103], BELLE [104, 105] and BABAR [106–108] give [6]

$$\text{Br}(\bar{B} \rightarrow X_s \gamma) = (3.49 \pm 0.19) \times 10^{-4}. \quad (25)$$

In the next numerical analysis, we use our previous work about the rare decay $\bar{B} \rightarrow X_s \gamma$ in the $\mu\nu\text{SSM}$ [109].

A. Muon MDM

Firstly, we analyze the muon MDM in the $\mu\nu\text{SSM}$. We define

$$R_a \equiv \frac{a_\mu^{\text{two-loop}}}{a_\mu^{\text{one-loop}}}, \quad (26)$$

to show the ratio of two-loop corrections to one-loop corrections of the the muon MDM. To present numerical analysis, we scan the parameter space shown in Tab. I. Here the steps are large, because the running of the program is not very fast. However, the scanning parameter space is broad enough to contain the possibility of more. Considered that the light stop mass is easily ruled out by the experiment, we scan the parameter $m_{\tilde{u}_3^c}$ from 1 TeV. In the scanning, The results are also constrained by the lightest Higgs boson mass with $124.68 \text{ GeV} \leq m_h \leq 125.52 \text{ GeV}$, the branching ratio of $\bar{B} \rightarrow X_s \gamma$ with $2.92 \times 10^{-4} \leq \text{Br}(\bar{B} \rightarrow X_s \gamma) \leq 4.06 \times 10^{-4}$ and the muon anomalous magnetic dipole moment with $3.7 \times 10^{-10} \leq \Delta a_\mu \leq 49.9 \times 10^{-10}$, where a 3σ experimental error is considered.

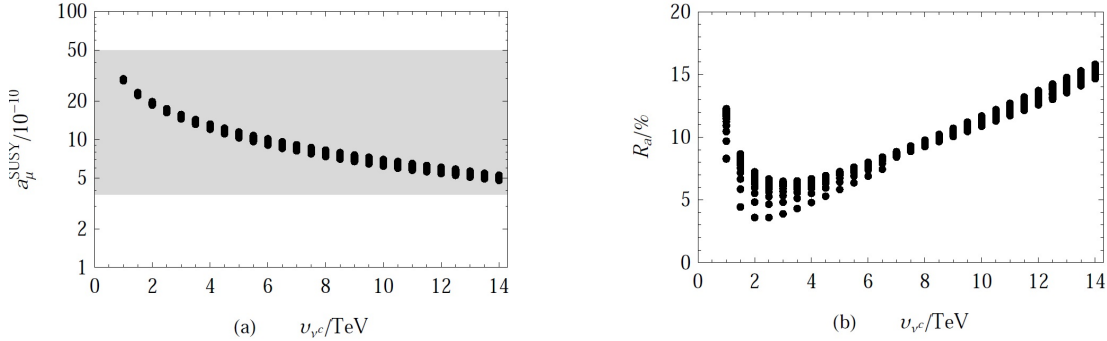


FIG. 2: a_μ^{SUSY} (a) and R_a (b) vary with v_{ν^c} , where the gray area denotes the muon MDM at 3.0σ .

Through scanning the parameter space shown in Tab. I, we can plot the muon anomalous MDM a_μ^{SUSY} and the ratio R_a varying with the parameter v_{ν^c} in Fig. 2, where the gray area denotes the muon MDM at 3.0σ given in Eq. (2). In Fig. 2(a), the numerical results show that the muon anomalous magnetic dipole moment a_μ^{SUSY} are decoupling with increasing v_{ν^c} , which coincides with the decoupling theorem. We can see that the value of the muon anomalous MDM a_μ^{SUSY} in the $\mu\nu$ S SM could reach the experimental center value shown in Eq. (2), when v_{ν^c} is small.

To show the two-loop contributions of the muon MDM, Fig. 2(b) pictures the ratio R_a varying with the parameter v_{ν^c} . Normalized to the one-loop corrections of the muon MDM, the ratio R_a can reach around 16% when v_{ν^c} is large. Here, when v_{ν^c} is large, the one-loop corrections of the muon MDM are decoupling quickly than the two-loop corrections. The numerical results also show that the ratio R_a can be about 12% when v_{ν^c} is small. Therefore, the two-loop Barr-Zee type corrections also make important contributions to the muon anomalous MDM in the $\mu\nu$ S SM.

To see the difference of two-loop contributions of muon MDM between the $\mu\nu$ S SM and the MSSM, we define

$$R_m \equiv \frac{(a_\mu^{two-loop})_{\mu\nu\text{SSM}} - (a_\mu^{two-loop})_{\text{MSSM}}}{(a_\mu^{two-loop})_{\text{MSSM}}}. \quad (27)$$

Here, $(a_\mu^{two-loop})_{\mu\nu\text{SSM}}$ and $(a_\mu^{two-loop})_{\text{MSSM}}$ respectively denote two-loop contribution of muon MDM of the $\mu\nu$ S SM and that of the MSSM, which can be given in Sec. IV. Through scanning the parameter space shown in Tab. I, we also picture Fig. 3 to show that R_m varies with v_{ν^c} and $\tan\beta$. In Fig. 3(a), we can see that the ratio R_m can reach about 27%, when v_{ν^c} is

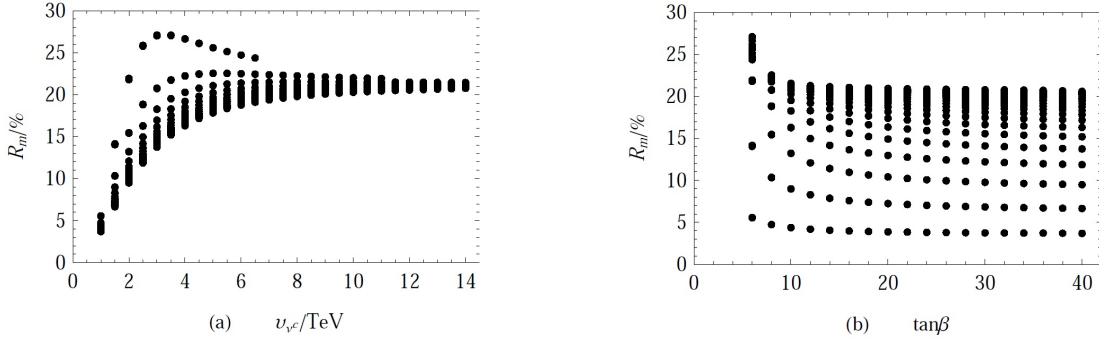


FIG. 3: R_m varies with $v_{\nu c}$ (a) and $\tan\beta$ (b).

Parameters	Min	Max	Step
$\tan\beta$	4	40	2
$v_{\nu c}/\text{TeV}$	1	14	0.5
M_2/TeV	0.4	4	0.2
$m_{\tilde{u}_3^c}/\text{TeV}$	1	4	0.3
A_t/TeV	1	4	0.3

TABLE II: Scanning parameters for the Higgs boson to $Z\gamma$ decay.

around 3 TeV. when the parameter $v_{\nu c}$ is large, the ratio R_m is tend to be stable and around 20%. In Fig. 3(b), we can know that when $\tan\beta$ is small, the ratio R_m can be large. Here, compared to the MSSM, the $\mu\nu$ SSM has extra right-handed neutrinos which can give new contributions. Simultaneously, the right-handed neutrino superfields lead to the mixing of right-handed neutrinos with the neutralinos.

B. The decay $h \rightarrow Z\gamma$

In this subsection, we present the numerical results of the signal strength for $h \rightarrow Z\gamma$. We scan the parameter space shown in Tab. II, which also consider the experimental constraints above. In Fig. 4(a), we plot the signal strength $\mu_{Z\gamma}^{\text{ggF}}$ varying with $\tan\beta$. The numerical results show that $0.9 \lesssim \mu_{Z\gamma}^{\text{ggF}} \lesssim 1.1$. When $\tan\beta = 6$, the signal strength $\mu_{Z\gamma}^{\text{ggF}}$ can be down to 0.90 and up to 1.05. Here, the lightest Higgs boson in the $\mu\nu$ SSM gets an additional term $\frac{2\lambda_i \lambda_i s_W^2 c_W^2}{e^2} m_Z^2 \sin 2\beta$ in Eq. (9), comparing with the MSSM. Thus, the lightest Higgs boson

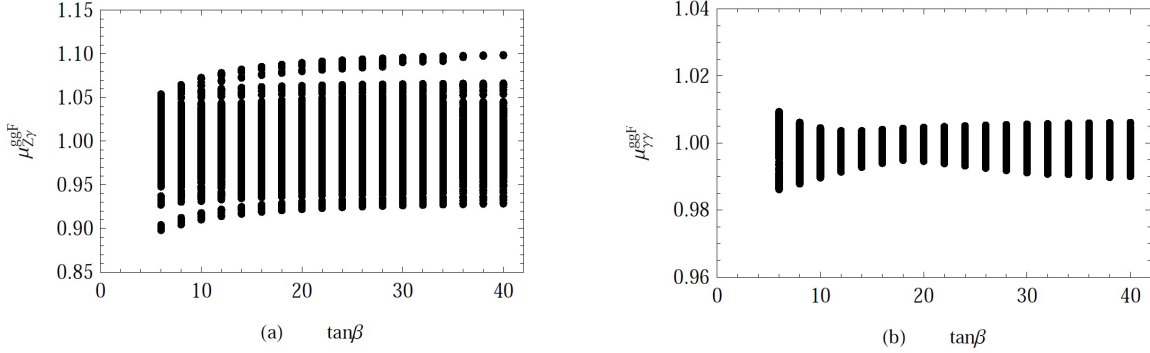


FIG. 4: The signal strength $\mu_{Z\gamma}^{\text{ggF}}$ (a) and $\mu_{\gamma\gamma}^{\text{ggF}}$ (b) versus $\tan\beta$.

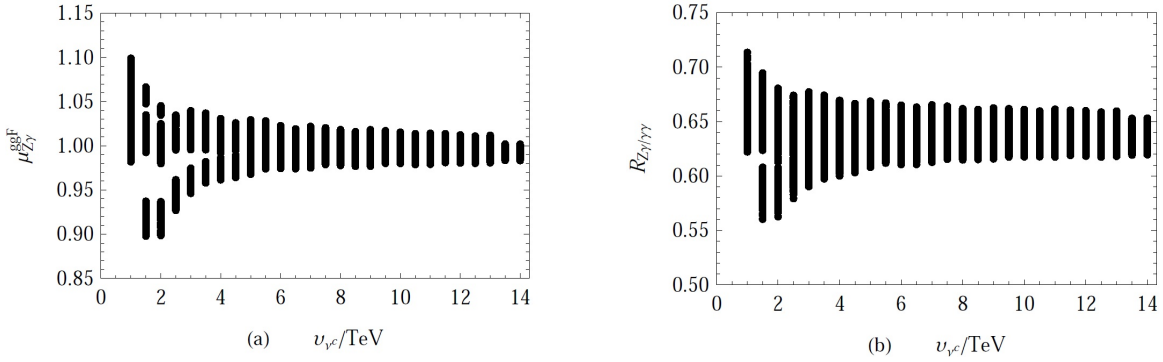


FIG. 5: The signal strength $\mu_{Z\gamma}^{\text{ggF}}$ (a) and the ratio $R_{Z\gamma/\gamma\gamma}$ (b) versus the parameter $v_{\nu c}$.

in the $\mu\nu$ SSM can easily account for the mass around 125 GeV, especially for small $\tan\beta$.

In Fig. 4(b), we also picture the signal strength $\mu_{\gamma\gamma}^{\text{ggF}}$ varying with $\tan\beta$. We can see that the signal strength $\mu_{\gamma\gamma}^{\text{ggF}}$ almost is around 1, which is consistent with the experimental value in the error range. Here, the relatively large stop mass and stau mass reduce the the signal strength $\mu_{\gamma\gamma}^{\text{ggF}}$. In Ref. [56], the signals of the Higgs boson decay channels $h \rightarrow \gamma\gamma$, $h \rightarrow VV^*$ ($V = Z, W$), and $h \rightarrow f\bar{f}$ ($f = b, \tau$) in the $\mu\nu$ SSM have been investigated. When the lightest stop mass $m_{\tilde{t}_1} \gtrsim 700$ GeV and the lightest stau mass $m_{\tilde{\tau}_1} \gtrsim 300$ GeV, the signal strengths of these Higgs boson decay channels are in agreement with the SM.

We plot the signal strength $\mu_{Z\gamma}^{\text{ggF}}$ versus the parameter $v_{\nu c}$ in Fig. 5(a). The numerical results present that the signal strength $\mu_{Z\gamma}^{\text{ggF}}$ can have a large deviation from 1, when the value of the parameter $v_{\nu c}$ is small. The parameter $v_{\nu c}$ directly affects the mass of chargino. The small chargino mass give a large contribution to the signal strength $\mu_{Z\gamma}^{\text{ggF}}$. In addition, the parameter $v_{\nu c}$ leads to the mixing of the neutral components of the Higgs doublets with

the sneutrinos. The mixing affects the lightest Higgs boson mass and the Higgs couplings, which is different from the MSSM.

To see more clearly, we also plot the ratio $R_{Z\gamma/\gamma\gamma} \equiv \Gamma_{\text{NP}}(h \rightarrow Z\gamma)/\Gamma_{\text{NP}}(h \rightarrow \gamma\gamma)$ versus the parameter v_{ν^c} in Fig. 5(b). We can see that $0.55 \lesssim R_{Z\gamma/\gamma\gamma} \lesssim 0.71$, when v_{ν^c} is small. Here, small value of the parameter v_{ν^c} gives more large contribution to the decay width $\Gamma_{\text{NP}}(h \rightarrow Z\gamma)$ than $\Gamma_{\text{NP}}(h \rightarrow \gamma\gamma)$. Thus, even though $\mu_{\gamma\gamma}^{\text{ggF}}$ is in accord with the SM, the signal strength $\mu_{Z\gamma}^{\text{ggF}}$ still has a large deviation from 1, through small value of the parameter v_{ν^c} which affects the mass of chargino and leads to the mixing of the neutral components of the Higgs doublets with the sneutrinos.

VI. SUMMARY

In the framework of the $\mu\nu$ SSM, the three singlet right-handed neutrino superfields $\hat{\nu}_i^c$ are introduced to solve the μ problem of the MSSM and generate three tiny Majorana neutrino masses at the tree level through seesaw mechanism. The gravitino or the axino in the $\mu\nu$ SSM also can be a dark matter candidate. The right-handed sneutrino VEVs lead to the mixing of the neutral components of the Higgs doublets with the sneutrinos. Therefore, the mixing would affect the lightest Higgs boson mass and the Higgs couplings, which gives a rich phenomenology in the Higgs sector of the $\mu\nu$ SSM, being different from the MSSM.

In this paper, we analyze the signal strength of the Higgs boson decay $h \rightarrow Z\gamma$ in the $\mu\nu$ SSM. Even though the signal strength of $h \rightarrow \gamma\gamma$ is in accord with the SM, the signal strength of $h \rightarrow Z\gamma$ still has a large deviation from 1, due to the small mass of chargino and the mixing of the neutral components of the Higgs doublets with the sneutrinos. The present observed 95% CL upper limit on the signal strength of the $h \rightarrow Z\gamma$ decay still is 6.6 [9]. However, high luminosity or high energy large collider [110–112] built in the future will detect the Higgs boson decay $h \rightarrow Z\gamma$.

Here, we also consider the two-loop Barr-Zee type corrections of muon anomalous MDM in the $\mu\nu$ SSM. Normalized to the one-loop corrections of the muon MDM, the two-loop Barr-Zee type corrections can be around 16%. Compared to the MSSM, the $\mu\nu$ SSM has extra right-handed neutrinos which can give new contributions. Therefore, the two-loop

Barr-Zee type corrections also make important contributions to the muon anomalous MDM in the $\mu\nu$ SSM. In near future, the Muon g-2 experiment at Fermilab [113, 114] will measure the muon anomalous magnetic dipole moment to unprecedented precision.

Acknowledgments

The work has been supported by the National Natural Science Foundation of China (NNSFC) with Grants No. 11535002, No. 11705045, the youth top-notch talent support program of the Hebei Province, and Midwest Universities Comprehensive Strength Promotion project.

Appendix A: FORM FACTORS

$$A_{1/2}(\tau, \lambda) = I_1(\tau, \lambda) - I_2(\tau, \lambda), \quad (\text{A1})$$

$$A_1(\tau, \lambda) = c_W \left\{ 4 \left(3 - \frac{s_W^2}{c_W^2} \right) I_2(\tau, \lambda) + \left[\left(1 + \frac{2}{\tau} \right) \frac{s_W^2}{c_W^2} - \left(5 + \frac{2}{\tau} \right) \right] I_1(\tau, \lambda) \right\}, \quad (\text{A2})$$

$$A_0(\tau, \lambda) = I_1(\tau, \lambda), \quad (\text{A3})$$

$$I_1(\tau, \lambda) = \frac{\tau\lambda}{2(\tau - \lambda)} + \frac{\tau^2\lambda^2}{2(\tau - \lambda)^2} [f(\tau^{-1}) - f(\lambda^{-1})] + \frac{\tau^2\lambda}{(\tau - \lambda)^2} [g(\tau^{-1}) - g(\lambda^{-1})], \quad (\text{A4})$$

$$I_2(\tau, \lambda) = -\frac{\tau\lambda}{2(\tau - \lambda)} [f(\tau^{-1}) - f(\lambda^{-1})], \quad (\text{A5})$$

$$f(\tau) = \begin{cases} \arcsin^2 \sqrt{\tau}, & \tau \leq 1; \\ -\frac{1}{4} \left[\ln \frac{1 + \sqrt{1-1/\tau}}{1 - \sqrt{1-1/\tau}} - i\pi \right]^2, & \tau > 1, \end{cases} \quad (\text{A6})$$

$$g(\tau) = \begin{cases} \sqrt{\tau^{-1} - 1} \arcsin \sqrt{\tau}, & \tau \geq 1; \\ -\frac{\sqrt{1-\tau^{-1}}}{2} \left[\ln \frac{1 + \sqrt{1-1/\tau}}{1 - \sqrt{1-1/\tau}} - i\pi \right], & \tau < 1. \end{cases} \quad (\text{A7})$$

-
- [1] G. Aad et al. (ATLAS Collaboration), *Phys. Lett.* **B 716** (2012) 1.
[2] S. Chatrchyan et al. (CMS Collaboration), *Phys. Lett.* **B 716** (2012) 30.
[3] G. Aad et al. (ATLAS and CMS Collaborations), *Phys. Rev. Lett.* **114** (2015) 191803.

- [4] A. M Sirunyan et al. (CMS Collaboration), *JHEP* **11** (2017) 047.
- [5] M. Aaboud et al. (ATLAS Collaboration), *Phys. Lett. B* **784** (2018) 345-366.
- [6] M. Tanabashi et al. (Particle Data Group), *Phys. Rev. D* **98** (2018) 030001, and 2019 update.
- [7] M. Aaboud et al. (ATLAS collaboration), *Phys. Lett. B* **732** (2014) 8-27.
- [8] A.M. Sirunyan et al. (CMS Collaboration), *Phys. Lett. B* **726** (2013) 587-609.
- [9] M. Aaboud et al. (ATLAS collaboration), *JHEP* **10** (2017) 112.
- [10] A.M. Sirunyan et al. (CMS Collaboration), *JHEP* **11** (2018) 152.
- [11] R.N. Cahn, M.S. Chanowitz, N. Fleishon, *Phys. Lett. B* **082** (1979) 113.
- [12] L. Bergstrom, G. Hulth, *Nucl. Phys. B* **259** (1985) 137.
- [13] J.F. Gunion, G.L. Kane, J. Wudka, *Nucl. Phys. B* **299** (1988) 231.
- [14] T.J. Weiler, T.-C. Yuan, *Nucl. Phys. B* **318** (1989) 337.
- [15] A. Djouadi, V. Driesen, W. Hollik, A. Kraft, *Eur. Phys. J. C* **1** (1998) 163-175.
- [16] A. Djouadi, *Phys. Rep.* **457** (2008) 1.
- [17] A. Djouadi, *Phys. Rep.* **459** (2008) 1.
- [18] M. Carena, I. Lowd, C.E.M. Wagner, *JHEP* **08** (2012) 060.
- [19] E. Masso, V. Sanz, *Phys. Rev. D* **87** (2013) 033001.
- [20] C.-W. Chiang, K. Yagyu, *Phys. Rev. D* **87** (2013) 033003.
- [21] C.-S. Chen, C.-Q. Geng, D. Huang, L.-H. Tsai, *Phys. Rev. D* **87** (2013) 075019.
- [22] A.Y. Korchin, V.A. Kovalchuk, *Phys. Rev. D* **88** (2013) 036009.
- [23] N. Maru, N. Okada, *Phys. Rev. D* **88** (2013) 037701.
- [24] C.-X. Yue, Q. -Y. Shi, T. Hua, *Nucl. Phys. B* **876** (2013) 747.
- [25] J. Cao, L. Wu, P. Wu, J.M. Yang, *JHEP* **09** (2013) 043.
- [26] Y. Chen, R. Harnik, R. Vega-Morales, *Phys. Rev. Lett.* **113** (2014) 191801.
- [27] G. Bélanger, V. Bizouard, G. Chalons, *Phys. Rev. D* **89** (2014) 095023.
- [28] Y. Chen, A. Falkowski, I. Low, R. Vega-Morales, *Phys. Rev. D* **90** (2014) 113006.
- [29] D. Fontes, J.C. Romao, J.P. Silva, *JHEP* **12** (2014) 043.
- [30] A. Hammad, S. Khalil, S. Moretti, *Phys. Rev. D* **92** (2015) 095008.
- [31] M. Farina, Y. Grossman, D.J. Robinson, *Phys. Rev. D* **92** (2015) 073007.
- [32] Q.-H. Cao, H.-R. Wang, Y. Zhang, *Chin. Phys. C* **39** (2015) 113102.

- [33] R. Bonciani, V.D. Duca, H. Frellesvig, J.M. Henn, F. Moriello, V.A. Smirnov, *JHEP* **08** (2015) 108.
- [34] T. Gehrmann, S. Guns, D. Kara, *JHEP* **09** (2015) 038.
- [35] A. Hammad, S. Khalil, S. Moretti, *Phys. Rev. D* **93** (2016) 115035.
- [36] J.M. No, M. Spannowsky, *Phys. Rev. D* **95** (2017) 075027.
- [37] X. Chen, G. Li, X. Wan, *Phys. Rev. D* **96** (2017) 055023.
- [38] J.M. Campbell, T. Neumann, C. Williams, *JHEP* **11** (2017) 150.
- [39] S.-M. Zhao, T.-F. Feng, J.-B. Chen, J.-J. Feng, G.-Z. Ning, H.-B. Zhang, *Phys. Rev. D* **97** (2018) 095043.
- [40] L.T. Hue, A. B. Arbuzov, T.T. Hong, T.P. Nguyen, D. T. Si, H.N. Long, *Eur. Phys. J. C* **78** (2018) 885.
- [41] A. Dedes, K. Suxho, L. Trifyllis, *JHEP* **06** (2019) 115.
- [42] H.T. Hung, T.T. Hong, H.H. Phuong, H.L.T. Mai, L.T. Hue, arXiv:1907.06735.
- [43] D.E. López-Fogliani and C. Muñoz, *Phys. Rev. Lett.* **97** (2006) 041801, hep-ph/0508297.
- [44] N. Escudero, D.E. López-Fogliani, C. Muñoz and R. Ruiz de Austri, *JHEP* **12** (2008) 099, arXiv:0810.1507.
- [45] J. Fidalgo, D.E. López-Fogliani, C. Muñoz and R. Ruiz de Austri, *JHEP* **10** (2011) 020, arXiv:1107.4614.
- [46] P. Bandyopadhyay, P. Ghosh and S. Roy, *Phys. Rev. D* **84** (2011) 115022, arXiv:1012.5762.
- [47] P. Ghosh, D.E. López-Fogliani, V.A. Mitsou, C. Muñoz and R. Ruiz de Austri, *Phys. Rev. D* **88** (2013) 015009, arXiv:1211.3177.
- [48] H.-B. Zhang, T.-F. Feng, G.-F. Luo, Z.-F. Ge and S.-M. Zhao, *JHEP* **07** (2013) 069 [*Erratum ibid.* **10** (2013) 173], arXiv:1305.4352.
- [49] H.-B. Zhang, T.-F. Feng, S.-M. Zhao and F. Sun, *Int. J. Mod. Phys. A* **29** (2014) 1450123, arXiv:1407.7365.
- [50] J.E. Kim and H.P. Nilles, *Phys. Lett. B* **138** (1984) 150.
- [51] H.P. Nilles, *Phys. Rept.* **110** (1984) 1.
- [52] H.E. Haber and G.L. Kane, *Phys. Rept.* **117** (1985) 75.
- [53] H.E. Haber, arXiv:hep-ph/9306207.

- [54] S.P. Martin, arXiv:hep-ph/9709356.
- [55] J. Rosiek, *Phys. Rev. D* **41** (1990) 3464 [hep-ph/9511250].
- [56] H.-B. Zhang, T.-F. Feng, F. Sun, K.-S. Sun, J.-B. Chen, and S.-M. Zhao, *Phys. Rev. D* **89** (2014) 115007, arXiv:1307.3607.
- [57] H.-B. Zhang, T.-F. Feng, S.-M. Zhao, Y.-L. Yan, F. Sun, *Chin. Phys. C* **4** (2017) 043106, arXiv:1511.08979.
- [58] H.-B. Zhang, T.-F. Feng, X.-Y. Yang, S.-M. Zhao, G.-Z. Ning, *Phys. Rev. D* **95** (2017) 075013, arXiv:1704.03388.
- [59] G.W. Bennett et al. (Muon g-2 Collaboration), *Phys. Rev. D* **73** (2006) 072003.
- [60] S.A. Abel, W.N. Cottingham, I.-B. Whittingham, *Phys. Lett. B* **259** (1991) 307.
- [61] T. Moroi, *Phys. Rev. D* **53** (1996) 6565 [*Erratum ibid.* **D 56** (1997) 4424].
- [62] J.L. Feng and K.T. Matchev, *Phys. Rev. Lett.* **86** (2001) 3480.
- [63] S. P. Martin and J. D. Wells, *Phys. Rev. D* **64** (2001) 035003.
- [64] R. Arnowitt, B. Dutta, and Y. Santoso, *Phys. Rev. D* **64** (2001) 113010.
- [65] R.A. Diaz, hep-ph/0212237.
- [66] T.-F. Feng, X.-Q. Li, L. Lin, J. Maalampi, H.-S. Song, *Phys. Rev. D* **73** (2006) 116001.
- [67] T.-F. Feng, L.-Sun and X.-Y. Yang, *Nucl. Phys. B* **800** (2008) 221, arXiv:0805.1122.
- [68] T.-F. Feng, L.-Sun and X.-Y. Yang, *Phys. Rev. D* **77** (2008) 116008, arXiv:0805.0653.
- [69] T.-F. Feng and X.-Y. Yang, *Nucl. Phys. B* **814** (2009) 101, arXiv:0901.1686.
- [70] X.-Y. Yang and T.-F. Feng, *Phys. Lett. B* **675** (2009) 43.
- [71] K. Cheung, O.C.W. Kong and J.S. Lee, *JHEP* **06** (2009) 020, arXiv:0904.4352.
- [72] S.-M. Zhao, T.-F. Feng, H.-B. Zhang, B.-Yan, X.-J. Zhan, *JHEP* **11** (2014) 119, arXiv:1405.7561.
- [73] G.De Conto, V. Pleitez, *JHEP* **05** (2017) 104.
- [74] J.-L. Yang, T.-F. Feng, Y.-L. Yan, W. Li, S.-M. Zhao, H.-B. Zhang, *Phys. Rev. D* **99** (2019) 015002, arXiv:1812.03860.
- [75] X.-X. Dong, S.-M. Zhao, H.-B. Zhang, T.-F. Feng, arXiv:1901.07701.
- [76] P. Ghosh and S. Roy, *JHEP* **04** (2009) 069, arXiv:0812.0084.
- [77] A. Bartl, M. Hirsch, S. Liebler, W. Porodc and A. Vicente, *JHEP* **05** (2009) 120,

- arXiv:0903.3596.
- [78] J. Fidalgo, D.E. López-Fogliani, C. Muñoz and R.R. de Austri, *JHEP* **08** (2009) 105, arXiv:0904.3112.
 - [79] P. Ghosh, P. Dey, B. Mukhopadhyaya and S. Roy, *JHEP* **05** (2010) 087, arXiv:1002.2705.
 - [80] D.E. López-Fogliani, arXiv:1004.0884.
 - [81] P. Ghosh, *J. Phys. Conf. Ser.* **259** (2010) 012063, arXiv:1010.2578.
 - [82] H.-B. Zhang, T.-F. Feng, L.-N. Kou and S.-M. Zhao, *Int. J. Mod. Phys. A* **28** (2013) 1350117, arXiv:1307.6284.
 - [83] K.-Y. Choi, D.E. López-Fogliani, C. Muñoz, R.R. de Austri, *JCAP* 1003 (2010) 028.
 - [84] G.A.Gómez-Vargas, M. Fornasa, F. Zandanel, A.J. Cuesta, C. Muñoz, F. Prada, G. Yepes, *JCAP* 1202 (2012) 001.
 - [85] A. Albert et al., *JCAP* 1410 (2014) 023.
 - [86] G.A. Gómez-Vargas, D.E. López-Fogliani, C. Muñoz, A. D. Perez, R.R. de Austri, *JCAP* 1703 (2017) 047.
 - [87] G.A. Gómez-Vargas, D.E. López-Fogliani, C. Muñoz, A.D. Perez, arXiv:1911.03191.
 - [88] G.A. Gómez-Vargas, D.E. López-Fogliani, C. Muñoz, A.D. Perez, arXiv:1911.08550.
 - [89] Bing-Lin Young, *Front. Phys.* 12(2), 121201 (2017).
 - [90] S. Heinemeyer, W. Hollik, and G. Weiglein, *Comput. Phys. Commun.* **124** (2000) 76-89, hep-ph/9812320.
 - [91] S. Heinemeyer, W. Hollik, and G. Weiglein, *Eur. Phys. J. C* **9** (1999) 343-366, hep-ph/9812472.
 - [92] G. Degrassi, S. Heinemeyer, W. Hollik, P. Slavich, and G. Weiglein, *Eur. Phys. J. C* **28** (2003) 133-143, hep-ph/0212020.
 - [93] M. Frank, T. Hahn, S. Heinemeyer, W. Hollik, H. Rzehak, and G. Weiglein, *JHEP* **02** (2007) 047, arXiv:hep-ph/0611326.
 - [94] T. Hahn, S. Heinemeyer, W. Hollik, H. Rzehak, and G. Weiglein, *Comput. Phys. Commun.* **180** (2009) 1426-1427.
 - [95] T. Hahn, S. Heinemeyer, W. Hollik, H. Rzehak, and G. Weiglein, *Nucl. Phys. Proc. Suppl.* **205-206** (2010) 152-157, arXiv:1007.0956.

- [96] T. Hahn, S. Heinemeyer, W. Hollik, H. Rzehak, and G. Weiglein, *Phys. Rev. Lett.* **112** (2014) 141801, arXiv:1312.4937.
- [97] H. Bahl and W. Hollik, *Eur. Phys. J. C* **76** (2016) 499, arXiv:1608.01880.
- [98] B.C. Allanach, *Comput. Phys. Commun.* **143** (2002) 305-331, hep-ph/0104145.
- [99] B.C. Allanach and M.A. Bernhardt, *Comput. Phys. Commun.* **181** (2010) 232-245, arXiv:0903.1805.
- [100] B.C. Allanach, P. Athron, L. Tunstall, A. Voigt, and A. Williams, *Comput. Phys. Commun.* **185** (2014) 2322-2339, arXiv:1311.7659.
- [101] W. Porod, *Comput. Phys. Commun.* **153** (2003) 275-315, hep-ph/0301101.
- [102] W. Porod and F. Staub, *Comput. Phys. Commun.* **183** (2012) 2458-2469, arXiv:1104.1573.
- [103] S. Chen et al. (CLEO Collaboration), *Phys. Rev. Lett.* **87** (2001) 251807.
- [104] A. Limosani et al. (BELLE Collaboration), *Phys. Rev. Lett.* **103** (2009) 241801.
- [105] T. Saito et al. (BELLE Collaboration), *Phys. Rev. D* **91** (2015) 052004.
- [106] B. Aubert et al. (BABAR Collaboration), *Phys. Rev. D* **77** (2008) 051103.
- [107] J. P. Lees et al. (BABAR Collaboration), *Phys. Rev. Lett.* **109** (2012) 191801.
- [108] J. P. Lees et al. (BABAR Collaboration), *Phys. Rev. D* **86** (2012) 052012.
- [109] H.-B. Zhang, G.-H. Luo, T.-F. Feng, S.-M. Zhao, T.-J. Gao, K.-S. Sun, *Int. J. Mod. Phys. A* **29** (2014) 1450196, arXiv:1409.6837.
- [110] R. Contino et al., CERN Yellow Rep. (2017) no.3, 255-440, CERN-TH-2016-113, arXiv:1606.09408.
- [111] G. Apollinari et al., CERN Yellow Rep. Monogr. 4 (2017) 1-516, CERN-2017-007-M.
- [112] CEPC Study Group, IHEP-CEPC-DR-2018-02, arXiv:1811.10545.
- [113] J. Grange et al. (Muon g-2 Collaboration), FERMILAB-FN-0992-E, arXiv:1501.06858.
- [114] Muon g-2 Collaboration (A. Keshavarzi for the collaboration), EPJ Web Conf. 212 (2019) 05003, arXiv:1905.00497.